Hindawi Publishing Corporation
Physics Research International
Volume 2012, Article ID 161572, 9 pages
doi:10.1155/2012/161572

Research Article

Closed-Aperture Z-Scan Analysis for Nonlinear Media with Saturable Absorption and Simultaneous Third- and Fifth-Order Nonlinear Refraction

Xiangming Liu[1,2] and Yasuo Tomita[1]

[1] *Department of Engineering Science, The University of Electro-Communications, 1-5-1 Chofugaoka, Chofu, Tokyo 182-8585, Japan*
[2] *Research Institute for Electronic Science, Hokkaido University, Souseitou, Kita 21, Nishi 10, Kita-ku, Sapporo 001-0021, Japan*

Correspondence should be addressed to Xiangming Liu, liuxm@es.hokudai.ac.jp

Received 11 May 2012; Accepted 9 July 2012

Academic Editor: Michael R. Gleeson

We present a theory of open- and closed-aperture Gaussian beam Z-scan for nonlinear optical materials with saturable absorption and high-order nonlinear refraction. We show that an approximate expression for a transmitted intensity through the nonlinear optical material is possible by means of the Adomian's decomposition method and the thin film approximation. The theory is applied to semiconductor CdSe quantum dot-polymer nanocomposite films. It is shown that the theory well explains measured results of open- and closed-aperture transmittances in the Z-scan setup. It is also shown that the nanocomposite film possesses simultaneous third- and fifth-order nonlinear refraction as well as saturable absorption of a homogeneously broadened type.

1. Introduction

A Z-scan technique originally developed by Sheik-Bahae et al. [1] has been widely used for characterizing the nonlinear optical properties of various nonlinear optical materials whose nonlinear optical responses include nonlinear absorption and nonlinear refraction. Nonlinear absorption may be classified into four types (1) two-photon absorption (TPA), (2) multiphoton absorption, (3) saturable absorption (SA), and (4) reverse SA. Nonlinear refraction includes the third- and higher-order nonlinear refraction as well as cascaded second-order nonlinear refraction. The original Z-scan theory treats nonlinear optical materials having either the third-order nonlinear refraction with TPA or the fifth-order nonlinear refraction without TPA. Later, the theory was extended to the open-aperture Z-scan theories for nonlinear optical materials having multiphoton absorption [2], simultaneous TPA and three-photon absorption [3], and SA [4]. In addition, Z-scan analyses for nonlinear optical materials having simultaneous third- and fifth-order nonlinear refraction with or without TPA [5–9] were reported previously. These extensions are important for materials characterization and device design of, for example, optical limiters and all-optical photonic devices using third- and high-order nonlinear optical effects. However, no Z-scan theory has been reported so far for nonlinear optical materials having both SA and simultaneous third and fifth-order nonlinear refraction. Such a new nonlinear optical phenomenon has been indeed observed in our recently developed inorganic-organic nanocomposites, semiconductor CdSe quantum-dot- (QD-) polymer nanocomposite films [10, 11]. This new class of inorganic-organic nanocomposite material is capable of optically constructing multidimensional and functional (e.g., nonlinear) photonic lattice structures by the so-called holographic assembly of nanoparticles [12]. Indeed, we recently demonstrated holographic assembly of semiconductor CdSe QDs in photopolymer for constructing volume Bragg grating structures with diffraction efficiency near 100% [10]. This composite material has potential nonlinear optical applications such as optical switching/limiting, signal/image processing, and nonlinear photonic crystals [13, 14].

The electronic states of QDs are strongly influenced by the quantum confinement effect when the radius of QDs is smaller than approximately three times of the exciton Bohr radius [15]. The band gap (E_g) of QDs increases with

decreasing their size and the quantum confinement effect can strongly enhance the third-order optical nonlinearity [16, 17]. The II-VI bulk semiconductor CdSe has the direct band gap $E_g = 1.74$ eV at 300 K and has the exciton Bohr radius of 5.6 nm [17]. Therefore, the strong quantum confinement effect of CdSe QDs plays an important role in a large enhancement of the optical nonlinearity as compared with that of the bulk CdSe. Most of past studies with semiconductor QDs reported the third-order optical nonlinearity with and without TPA, although high-order optical nonlinearities in CdS_xSe_{1-x} QDs doped glasses [18–20] and colloidal CdTe QDs [21] were also reported. Saturation of the cubic Kerr nonlinearity due to high-order nonlinearities prominently at high optical intensities provides interesting nonlinear phenomena such as the formation of stable multidimensional optical solitons, but it sometimes causes a detrimental effect [22]. Therefore, it is necessary to characterize the third- and, if any, high-order optical nonlinearities in nanocomposite materials.

In this paper, we present a theory of the open and closed-aperture Gaussian beam Z-scan for nonlinear optical materials with both SA and simultaneous third- and fifth-order nonlinear refraction. We show that an approximate expression for a transmitted intensity through a nonlinear optical material possessing SA can be found by means of the Adomian's decomposition method [23]. The theory is applied to semiconductor CdSe QD-polymer nanocomposite films. It is shown that the theory well explains measured results of open- and closed-aperture transmittances in the Z-scan setup. It is also shown that the nanocomposite film possesses simultaneous third- and fifth-order nonlinear refraction as well as SA of a homogeneously broadened type.

2. Theory

Consider a single transverse mode Gaussian beam propagating along the z direction in a thin nonlinear medium of thickness L with SA of a homogeneously broadened type. In this case the intensity-dependent absorption coefficient $\alpha(I)$ is given by

$$\alpha(I) = \frac{\alpha_0}{1 + I/I_s}, \tag{1}$$

where α_0 is the linear absorption coefficient and I_s is the saturable intensity. Note that the intensity I is a function of the radial distance r from the beam axis, time t, the propagation distance z from the Gaussian beam spot, and the local distance $z'(0 \le z' \le L)$ measured from the entrance surface of the medium can be decomposed by means of the Adomian's decomposition method [23] and is given in a polynomial form as [4]

$$I(r, z, z', t) = I_{\text{in}}\left[1 + \sum_{n=1}^{\infty} \frac{(-\alpha_0 z')^n}{n!} \frac{g_n(\eta)}{(1+\eta)^{2n-1}}\right], \tag{2}$$

where $\eta = I_{\text{in}}/I_s$ in which the incident intensity I_{in} is given by

$$I_{\text{in}}(r, z, t) = \frac{I_0(t)}{1 + (z/z_0)^2} \exp\left[-\frac{2r^2}{w^2(z)}\right], \tag{3}$$

with $I_0(t)$ being the on-axis input intensity in the medium at the beam focus, which contains the temporal intensity envelope peaked at $t = 0$, and $w^2(z) = w_0{}^2(1 + z^2/z_0{}^2)$. Here, w_0 is the beam waist radius and z_0 is the diffraction length given by $kw_0{}^2/2$ with k being the wavenumber of the incident beam. We therefore note that η is a function of z, r, and t. The first eight terms of $g_n(\eta)$ in (2), which are numerically confirmed to approximately represent a solution given by (2) with a high accuracy, are given by

$$\begin{aligned}
g_1(\eta) &= 1,\\
g_2(\eta) &= 1,\\
g_3(\eta) &= 1 - 2\eta,\\
g_4(\eta) &= 1 - 8\eta + 6\eta^2,\\
g_5(\eta) &= 1 - 22\eta + 58\eta^2 - 24\eta^3,\\
g_6(\eta) &= 1 - 52\eta + 328\eta^2 - 444\eta^3 + 120\eta^4,\\
g_7(\eta) &= 1 - 114\eta + 1452\eta^2 - 4400\eta^3 + 3708\eta^4 - 720\eta^5,\\
g_8(\eta) &= 1 - 240\eta + 5610\eta^2 - 32120\eta^3 + 58140\eta^4\\
&\quad - 33984\eta^5 + 5040\eta^6.
\end{aligned} \tag{4}$$

When the third- and fifth-order nonlinear refraction is taken into account (these contributions are sufficient for our experiment with semiconductor CdSe QD-polymer nanocomposite films as is shown later), the nonlinear phase shift $\Delta\phi$ under the thin film and slowly varying envelope approximations is found from the following differential equation [6, 9]:

$$\frac{d\Delta\phi}{dz'} = k\Delta n(I) = k(n_2 + n_4 I)I, \tag{5}$$

where n_2 and n_4 are the third- and fifth-order nonlinear refraction coefficients, respectively. Integration of (5) yields to the nonlinear phase shift given by

$$\begin{aligned}
\Delta\phi(r, z, t) &= kn_2 \int_0^L I(r, z, z', t)dz' + kn_4 \int_0^L I^2(r, z, z', t)dz'\\
&= \Delta\phi^{(3)}(r, z, t) + \Delta\phi^{(5)}(r, z, t),
\end{aligned} \tag{6}$$

where the third- and fifth-order nonlinear phase shifts, $\Delta\phi^{(3)}(r, z, t)$ and $\Delta\phi^{(5)}(r, z, t)$ are expressed as

$$\begin{aligned}
\Delta\phi^{(3)}(r, z, t) &= n_2 k L I_{\text{in}} A^{(3)}(r, z, t),\\
\Delta\phi^{(5)}(r, z, t) &= n_4 k L (I_{\text{in}})^2 A^{(5)}(r, z, t),
\end{aligned} \tag{7}$$

in which

$$A^{(3)}(r,z,t) = \left[1 + \sum_{n=1}^{\infty} \frac{(-\alpha_0 L)^{n+1}}{(n+1)!} \frac{g_n(\eta)}{(1+\eta)^{2n-1}}\right], \tag{8a}$$

$$A^{(5)}(r,z,t) = \left[1 + 2\sum_{n=1}^{\infty} \frac{(-\alpha_0 L)^{n+1}}{(n+1)!} \frac{g_n(\eta)}{(1+\eta)^{2n-1}} + \sum_{m=1}^{\infty}\sum_{n=1}^{\infty} \frac{(-\alpha_0 L)^{n+m+1}}{(m+n+1)m!n!} \frac{g_m(\eta)g_n(\eta)}{(1+\eta)^{2m+2n-2}}\right]. \tag{8b}$$

The electric field $E_e(r,z,t)$ at the exit surface of the medium that experiences the nonlinear phase shift is given by

$$E_e(r,z,t) = \sqrt{I(r,z,L,t)}\exp[i\Delta\phi(r,z,t)]. \tag{9}$$

The expansion of the exponential term on the right-hand side of (9) in a Taylor series yields to

$$e^{i\Delta\phi(r,z,t)} = \sum_{m=0}^{\infty} \frac{\left[i\sum_{n=1}^{2}\phi^{(2n+1)}(r,z,t)\right]^m}{m!} \cong \sum_{m=0}^{\infty} \frac{\left\{i\sum_{n=1}^{2}\Delta\varphi^{(2n+1)}(z,t)\exp[-(2nr^2)/(w^2(z))]\right\}^m}{m!}, \tag{10}$$

where

$$\Delta\varphi^{(2n+1)}(z,t) = n_{2n}kL\left[I^{\text{in}}(0,z,t)\right]^n A^{(2n+1)}(0,z,t). \tag{11}$$

In the second equation on the right-hand side of (10), the approximation is made such that (8a) and (8b) are evaluated at $r = 0$. Since $|\Delta\phi^{(3)}| \gg |\Delta\phi^{(5)}|$ in practice, the quadratic- and higher-order terms in $\Delta\phi^{(5)}$ for the expansion of (10) may be neglected. Then, using the treatment by Tsigaridas et al. [6] with the Gaussian decomposition method [1], the electric field of the transmitted Gaussian beam at the distance d from the medium exit plane is expressed as

$$E_a(r,z,t) = \sqrt{I(0,z,L,t)}\sum_{m=1}^{\infty}\left\{\frac{\left[i\Delta\varphi^{(3)}(z,t)\right]^m}{m!}E^{(m3)}(r,d) + \frac{mi^m}{m!}\left[\Delta\varphi^{(3)}(z,t)\right]^{m-1} \times \Delta\varphi^{(5)}(z,t)E^{(m5)}(r,d)\right\}, \tag{12}$$

where the electric field of each individual Gaussian beam propagated at the distance d is given by

$$E^{(m3,5)}(r,d) = F^{(m3,5)}\frac{w_0^{(m3,5)}}{w^{(m3,5)}(d)}\exp\left[-\left(\frac{r}{w^{(m3,5)}(d)}\right)^2\right] \times \exp\left(-\frac{ikr^2}{2R^{(m3,5)}(d)}\right) \times \exp\left[-ik(z+d) + i\left(\theta^{(m3,5)}(d) + \gamma^{(m3,5)}\right)\right]. \tag{13}$$

In (13),

$$w_0^{(m3,5)} = \left(\frac{2z_R^{(m3,5)}}{k}\right)^{1/2},$$

$$w^{(m3,5)}(d) = w_0^{(m3,5)}\left[1 + \left(\frac{D^{(m3,5)}+d}{z_R^{(m3,5)}}\right)^2\right]^{1/2},$$

$$R^{(m3,5)}(d) = \left(D^{(m3,5)}+d\right)\left[1 + \left(\frac{z_R^{(m3,5)}}{D^{(m3,5)}+d}\right)^2\right],$$

$$\theta^{(m3,5)}(d) = \tan^{-1}\left(\frac{D^{(m3,5)}+d}{z_R^{(m3,5)}}\right), \tag{14}$$

$$F^{(m3,5)} = \left[1 + \left(\frac{D^{(m3,5)}}{z_R^{(m3,5)}}\right)^2\right]^{1/2},$$

$$\gamma^{(m3,5)} = \tan^{-1}\left(\frac{z}{z_R^{(m3,5)}}\right) - \tan^{-1}\left(\frac{D^{(m3,5)}}{z_R^{(m3,5)}}\right),$$

where

$$z_R^{(m3,5)} = \frac{A^{(m3,5)}R^2(z)}{\left(A^{(m3,5)}\right)^2 + R^2(z)},$$

$$D^{(m3,5)} = \frac{\left(A^{(m3,5)}\right)^2 R(z)}{\left(A^{(m3,5)}\right)^2 + R^2(z)}, \tag{15}$$

in which

$$A^{(m3)} = \frac{k}{2}\frac{w^2(z)}{2m+1},$$

$$A^{(m5)} = \frac{k}{2}\frac{w^2(z)}{2m+3}, \tag{16}$$

$$R(z) = z\left[1 + \left(\frac{z_0}{z}\right)^2\right].$$

Note that the physical meanings of the parameters shown above are described in [6]. The normalized Z-scan transmittance $T(z)$ [1] is defined as

$$T(z) = \frac{\int_{-\infty}^{\infty} P_T(z,t)dt}{S\int_{-\infty}^{\infty} P_i(t)dt}, \tag{17}$$

where the transmitted power $P_T(z,t)$ through the aperture is given by

$$P_T(z,t) = 2\pi \int_0^{r_a} |E_a(r,z,t)|^2 r\, dr, \tag{18}$$

the input power $P_i(t)$ is expressed as $\pi\omega_0^2 I_0(t)/2$, and the linear transmittance of the aperture S is given by $1 - \exp(-2r_a^2/w_a^2)$ with r_a and w_a being the aperture radius and the Gaussian beam radius at the aperture, respectively. Note that although we have described the theory for SA of a homogeneously broadened type given by (1), it is also possible to analyze this problem for SA of an inhomogeneously broadened type.

In what follows, we show numerical calculations for $T(z)$ of the closed-aperture Z-scan for a nonlinear medium possessing both SA of a homogeneously broadened type and the simultaneous third- and fifth-order nonlinear refraction. Figure 1 shows $T(z)$ with n_2 and n_4 having the same signs for negative (positive) value for n_2 as shown in Figure 1(a) (Figure 1(b)), where the third- and fifth-order nonlinear phase shifts at the temporally and spatially peak input intensity $I_0(0)$ are defined as $\Delta\phi_0^{(3)} = n_2 k L I_0(0)$ and $\Delta\phi_0^{(5)} = n4kLI_0(0)^2$, respectively. It can be seen from Figures 1(a) and 1(b) that, unlike the pure third-order case, the peak-to-valley (or the valley-to-peak) configuration becomes asymmetric and its peak-to-valley difference in $T(z)$ increases with an increase in $|\Delta\phi_0^{(5)}|$ because n_2 and n_4 have the same signs. It can also be seen that the fifth-order effect separates the valley more than the peak. The single peak and valley configuration is always maintained although the symmetry of the configuration is opposite each other for $n_2 > 0$ and $n_2 < 0$. The deviation of the valley fromunity is larger than that of the peak with an increase in $|\Delta\phi_0^{(5)}|$. The peak and valley tend to approach to the beam waist position ($z = 0$) with an increase in $|\Delta\phi_0^{(5)}|$ as seen in Figures 1(a) and 1(b).

Figure 2 presents $T(z)$ with $\Delta\phi_0^{(3)}$ and $\Delta\phi_0^{(5)}$ having the opposite signs for negative (positive) value for n_2 as shown in Figure 2(a) (Figure 2(b)). It can be seen from Figures 2(a) and 2(b) that the peak-to-valley (or the valley-to-peak) configuration becomes asymmetric and its peak-to-valley difference in $T(z)$ decreases with an increase in $|\Delta\phi_0^{(5)}|$ because n_2 and n_4 have the opposite signs. It can also be seen that the fifth-order effect separates the valley more than the peak as similar to the case of the same signs of n_2 and n_4. The single peak and valley configuration is always maintained although the symmetry of the configuration is opposite each other. This trend is also the same as the case of the same signs of n_2 and n_4 for $n_2 > 0$ and $n_2 < 0$. The peak and valley tend to separate from the beam waist position ($z = 0$) with an increase in $|\Delta\phi_0^{(5)}|$ as seen in Figures 2(a) and 2(b). This trend is opposite to the case of the same signs of n_2 and n_4 shown in Figures 1(a) and 1(b).

Peak-to-valley differences in $T(z)$, $\Delta T_{p\text{-}v}$, are plotted as a function of $I_0(0)/I_s$ in Figure 3 for different values of $\Delta\phi_0^{(5)}$ when $T(z)$ maintains the single peak and valley configuration. It can be seen that $\Delta T_{p\text{-}v}$ with $n_2 = -5.0 \times 10^{-3}$ cm^2/GW and $n_4 = -1.0 \times 10^{-3}$ cm^4/GW^2 increases faster than the case of the pure third-order effect without the influence of the fifth-order effect with an increase in $I_0(0)/I_s$. On the other hand, the fifth-order effect results in a slow increase of $\Delta T_{p\text{-}v}$ as $I_0(0)/I_s$ increases with $n_2 = -5.0 \times 10^{-3}$ cm^2/GW and $n_4 = 1.0 \times 10^{-3}$ cm^4/GW^2.

A dependence of the normalized transmittance on S is shown in Figure 4. The calculation was made with $\Delta\phi_0^{(3)} = -0.5$ and $\Delta\phi_0^{(5)} = 0.1$ and at $I_0\,(0)/I_s = 0.33$. It can be seen that the peaks and valleys of $T(z)$ decrease as S increases. It means that the closed-aperture Z-scan is highly sensitive when S is small as reported in [1].

3. Application to Semiconductor Quantum Dot-Polymer Nanocomposites

3.1. Sample Preparation. CdSe QDs (the average core size of 3 nm) were synthesized by the aqueous synthetic method and then extracted into an ionic liquid monomer. Detailed descriptions of preparation for the CdSe QD-monomer syrup were given in [10]. The syrup was cast on a glass plate loaded with a 10-μm spacer and was covered with another glass plate. For our Z-scan measurement, this uncured film sample was exposed to a green LED to prepare a uniformly cured polymer nanocomposite film sample having the quantum-confined electron-hole transition at ~480 nm.

3.2. Experimental Setup. A conventional Z-scan technique [1] was employed to evaluate nonlinear absorption and nonlinear refraction of our uniformly cured polymer nanocomposite film samples. We used a frequency-doubled, passively and actively mode-locked Nd:YAG laser (Continuum, YG601) with the FWHM pulse width of 35 ps at a wavelength of 532 nm and at a repetition rate of 10 Hz. The incident laser beam was divided into two beams. One laser beam was taken as a reference, while the other one was focused onto the film sample by a 200 mm convex lens to a spot with its beam waist radius ~32 μm. A film sample was moved along the beam propagation direction (z-axis) by a computer-controlled moving stage. An aperture and a detector were placed at a distance far away from a film sample. Linear transmittance of the aperture S was set to be 0.06 in the closed-aperture Z-scan setup. Individual transmitted pulses at a given pulse energy within ±10% were selected and averaged to obtain one data point.

3.3. Experimental Results. Typical open-aperture Z-scan results for a film sample with 0.91 vol.% CdSe QDs at $I_0 = 0.6$, 1.2, and 1.8 GW/cm^2 are shown in Figures 5(a), 5(b), and 5(c). It can be seen that $T(z)$ is peaked at the beam focus. Since no nonlinear absorption was observed in a neat polymer film without CdSe QDs, the observed data was caused by the optical nonlinearity of CdSe QDs. The open Z-scan model with SA of a homogeneously broadened type [4] can clearly fit the data better than with TPA [1] having a negative TPA coefficient β. We note that the model with SA of an inhomogeneously broadened type could not fit well with the closed-aperture Z-scan data (not shown here). Figure 5(d) shows transmittance change $\Delta T(0)$ at $z = 0$ as a function

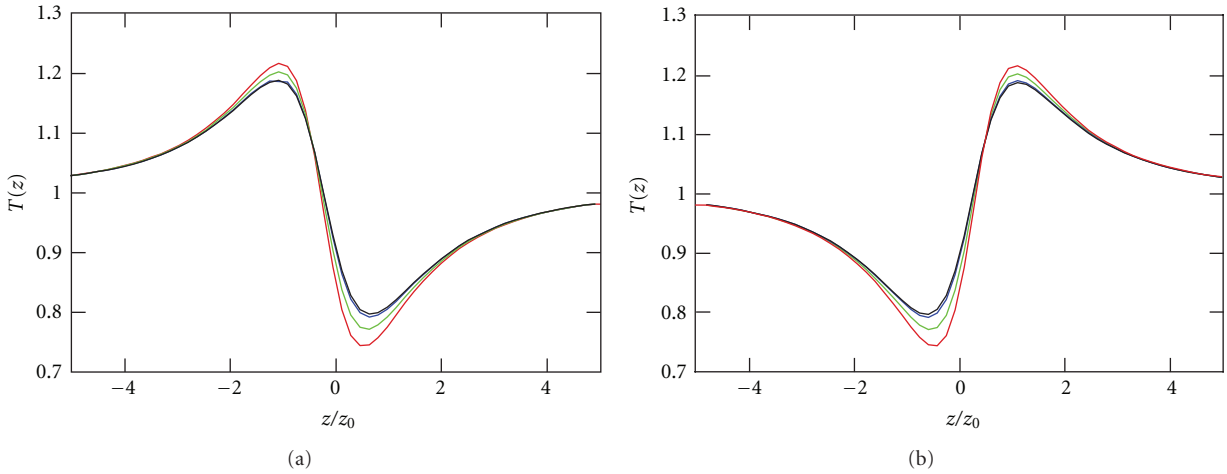

FIGURE 1: Normalized transmittances $T(z)$ with $S = 0.05$ and $I_s = 0.3\,\text{GW/cm}^2$ for (a) $\Delta\phi_0^{(3)} = -0.3\pi$ and $\Delta\phi_0^{(5)} < 0$ and (b) $\Delta\phi_0^{(3)} = 0.3\pi$ and $\Delta\phi_0^{(5)} > 0$. Solid curves in black, blue, green, and red correspond to $|\Delta\phi_0^{(5)}| = 0, 0.01\pi, 0.05\pi$ and 0.1π, respectively.

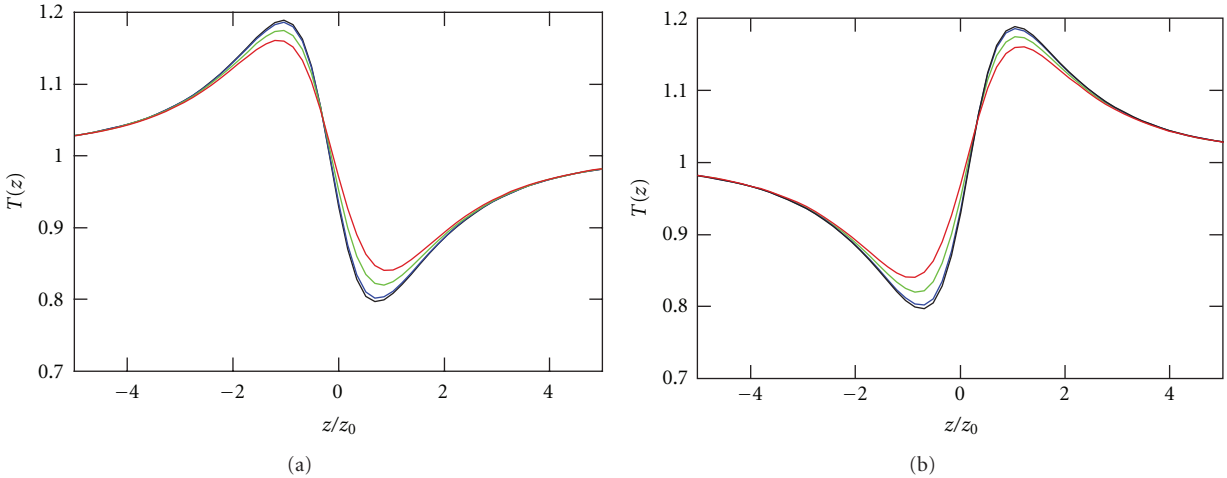

FIGURE 2: Normalized transmittances $T(z)$ with $S = 0.05$ and $I_s = 0.3\,\text{GW/cm}^2$ for (a) $\Delta\phi_0^{(3)} = -0.3\pi$ and $\Delta\phi_0^{(5)} > 0$ and (b) $\Delta\phi_0^{(3)} = 0.3\pi$ and $\Delta\phi_0^{(5)} < 0$. Solid curves in black, blue, green, and red correspond to $|\Delta\phi_0^{(5)}| = 0, 0.01\pi, 0.05\pi$ and 0.1π, respectively.

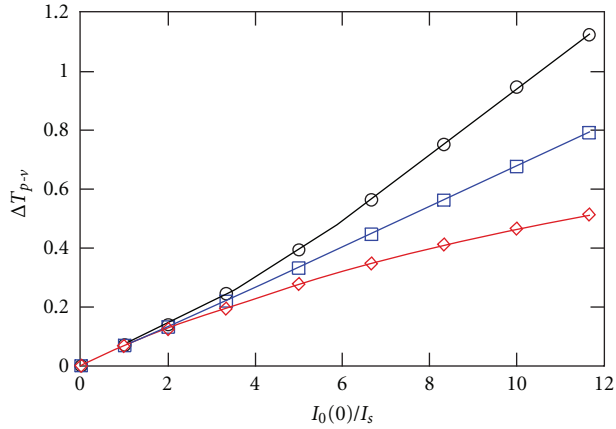

FIGURE 3: $\Delta T_{p\text{-}v}$ versus $I_0(0)/I_s$ for $S = 0.05$ and $I_s = 0.3\,\text{GW/cm}^2$ for $n_2 = -5.0 \times 10^{-3}\,\text{cm}^2/\text{GW}$ and $n_4 = 0$ (□), 1.0×10^{-3} (◇) and -1.0×10^{-3} (○) cm^4/GW^2. The solid curves are a guide to the eyes.

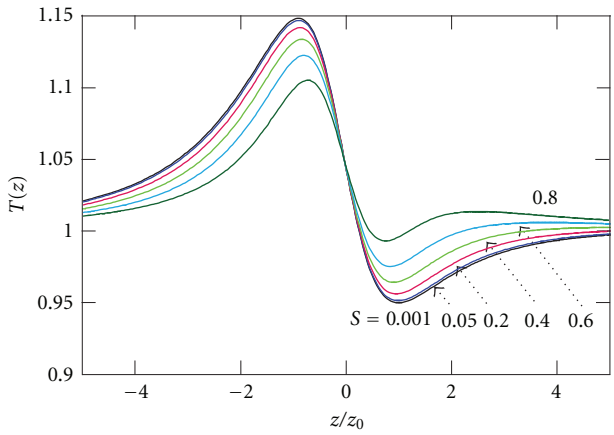

FIGURE 4: Normalized transmittances $T(z)$ for different aperture size S with $\Delta\phi_0^{(3)} = -0.5$ and $\Delta\phi_0^{(5)} = 0.1$ and at $I_0(0)/I_s = 0.33$.

of I_0. It can be seen that the SA model gives the best fit value for I_s to be 0.54 GW/cm^2, which is consistent with that (0.53 ± 0.06 GW/cm^2) estimated from Figures 5(a)–5(c). It follows that the saturable absorption observed in our film sample is well described by SA of a homogeneously broadened type. This result implies excellent size uniformity of CdSe QDs in our sample as confirmed by a transmission electron microscope image of CdSe QDs [11]. We consider that the physical origin of the light-induced transparency is caused by transient bleaching of the CdSe QDs [24].

Figure 6 shows the closed-aperture Z-scan result for the same film sample as that shown in Figure 5 at $I_0 = 1.8$ GW/cm^2, which is fitted by our closed-aperture Z-scan model without and with the fifth-order nonlinear refraction in the absence of nonlinear absorption (Figure 6(a)) and in the presence of saturable absorption (Figure 6(b)). It can be clearly seen from Figures 6(a) and 6(b) that the film sample exhibits the simultaneous third- and fifth-order nonlinear refraction as well as saturable absorption.

Figures 7(a), 7(b), and 7(c) show the closed-aperture Z-scan results at several levels of intensities for the same film sample as that shown in Figure 5. It can be seen that the Z-scan data exhibit the peak-and-valley configuration, indicating the negative nonlinear refraction. It is well known that $\Delta T_{p\text{-}v}$ is proportional to I_0 for a Kerr material [1]. However, we found that $\Delta T_{p\text{-}v}/I_0$ for our film sample approximately had a linear dependence of I_0 (see Figure 7(d)), indicating that the third-order effect was not the sole contribution to the observed optical nonlinearity. The fifth-order contribution to $T(z)$ as well as SA should be taken into account in the analysis of the closed-aperture Z-scan data.

Based on our model given in Section 2, we performed the curve fitting of the present theoretical model with I_s, together with n_2 and n_4 as fitting parameters, to the data. The best-fit values for n_2 and n_4 were found to be $(-4.0 \pm 0.6) \times 10^{-3}$ cm^2/GW and $(1.5 \pm 0.4) \times 10^{-3}$ cm^4/GW^2, respectively. For comparison, a theoretical fitting curve in which only third- and fifth-order nonlinear refraction is taken into account (without nonlinear absorption) is also shown in Figure 7. Poor fit with the data is obvious, showing the need for the inclusion of nonlinear absorption (i.e., SA in our case).

The magnitude of the obtained n_2 for the film sample with 0.91 vol.% (3.6 wt%) CdSe QDs is approximately two orders of magnitude larger than that (-1.45×10^{-5} cm^2/GW) of a bulk CdSe at 1064 nm [25] and is approximately one order of magnitude larger than that (4.3×10^{-4} cm^2/GW) at 794 nm for a polymer CR39 composite film with 1.5 wt% CdSe QDs [26]. Generally, electronic and thermal effects mainly contribute to the optical nonlinearities. However, the thermal contribution to the observed optical nonlinearities of the film sample was negligible in our experiment using a picosecond laser at a low repetition rate and therefore the dominating nonlinear response is attributed to the electronic origin as was also confirmed by degenerating multiwave mixing (DMWM) [11]. We also found from a dependence of n_4 on the concentration of CdSe QDs that the observed fifth-order nonlinearity had contributions mainly from the intrinsic fifth-order optical nonlinearity and partly from macroscopic and microscopic cascaded fifth-order optical nonlinearities [11, 27]. The occurrence of the intrinsic fifth-order optical nonlinearity is attributed to TPA-induced free carriers in bulk semiconductors [25]. In our case, however, it may originate from the state filling effect in CdSe QDs.

4. Conclusion

We have developed a closed-aperture Z-scan theory for nonlinear optical materials with SA of a homogeneously broadened type and with simultaneous third- and fifth-order nonlinear refraction. The shape and symmetry of the closed-aperture Z-scan transmittance are strongly influenced by the relative sign and magnitude of the fifth-order optical nonlinearity with respect to the third-order one. Because the light-induced transparency takes place due to SA, the peak (the valley) increases (decreases) in the closed-aperture Z-scan transmittance. The theoretical model has been applied to characterize the nonlinear optical properties of our newly developed uniformly cured CdSe QD-polymer nanocomposites. We have shown that the films exhibit SA as well as the negative third-order and the positive fifth-order nonlinear refraction. Such coexistence of the third- and fifth-order optical nonlinearities has also been confirmed by our recent DMWM measurements [11]. Finally, it should be stressed that the Z-scan theory presented in this paper is proved to be useful for characterizing the nonlinear optical properties of novel QD-polymer nanocomposite materials capable of constructing nonlinear photonic crystal structures by holographic patterning. In addition, the observed large nonlinear refraction and induced transparency as well as the capability of holographic nanoparticle assembling make QD-polymer nanocomposite materials promising for nonlinear photonics applications (e.g., optical switching, limiting, and signal processing) by use of holographic Bragg grating structures that provide the electromagnetic nonlinear feedback mechanism.

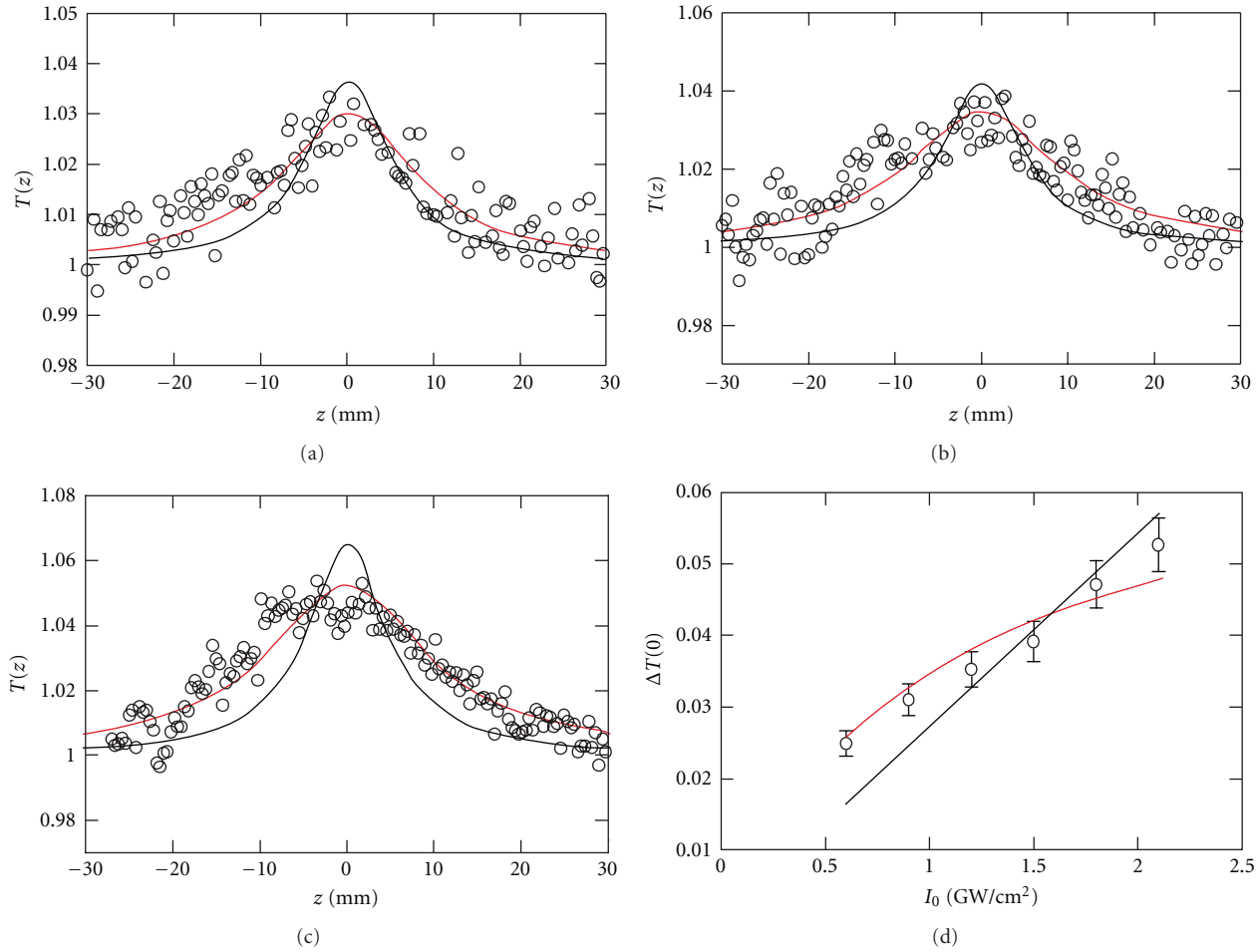

FIGURE 5: (a) Open-aperture Z-scan $T(z)$ at I_0 = (a) 0.6, (b) 1.2, and (c) 1.8 GW/cm^2 for a film sample with 0.91 vol.% CdSe QDs. (b) Transmittance change $\Delta T(0)$ at $z = 0$ as a function of input intensity I_0. The best fittings correspond to the SA (red) and TPA (black) models, respectively.

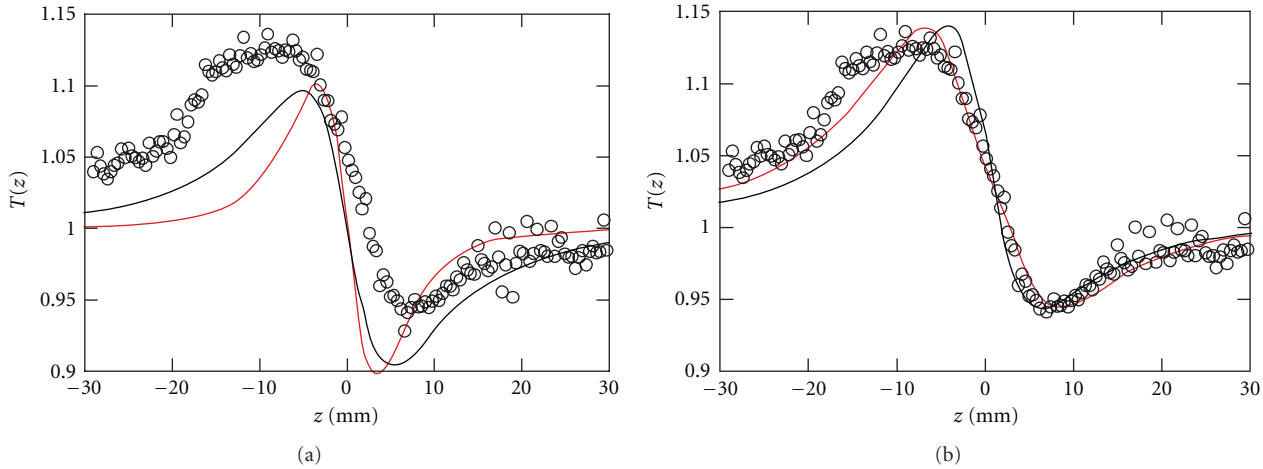

FIGURE 6: Closed-aperture Z-scan $T(z)$ at $I_0 = 1.8$ GW/cm^2 for the same film sample as that shown in Figure 5. In Figure 6(a), solid curves correspond to the least-squares fit of the theoretical formulae for a medium possessing the third-order nonlinear refraction without (black) and with (red) the fifth-order nonlinear refraction in the absence of saturable absorption of a homogeneously broadened type. In Figure 6(b), solid curves correspond to the least-squares fit for a medium possessing the third-order nonlinear refraction without (black) and with (red) the fifth-order nonlinear refraction in the presence of saturable absorption of a homogeneously broadened type.

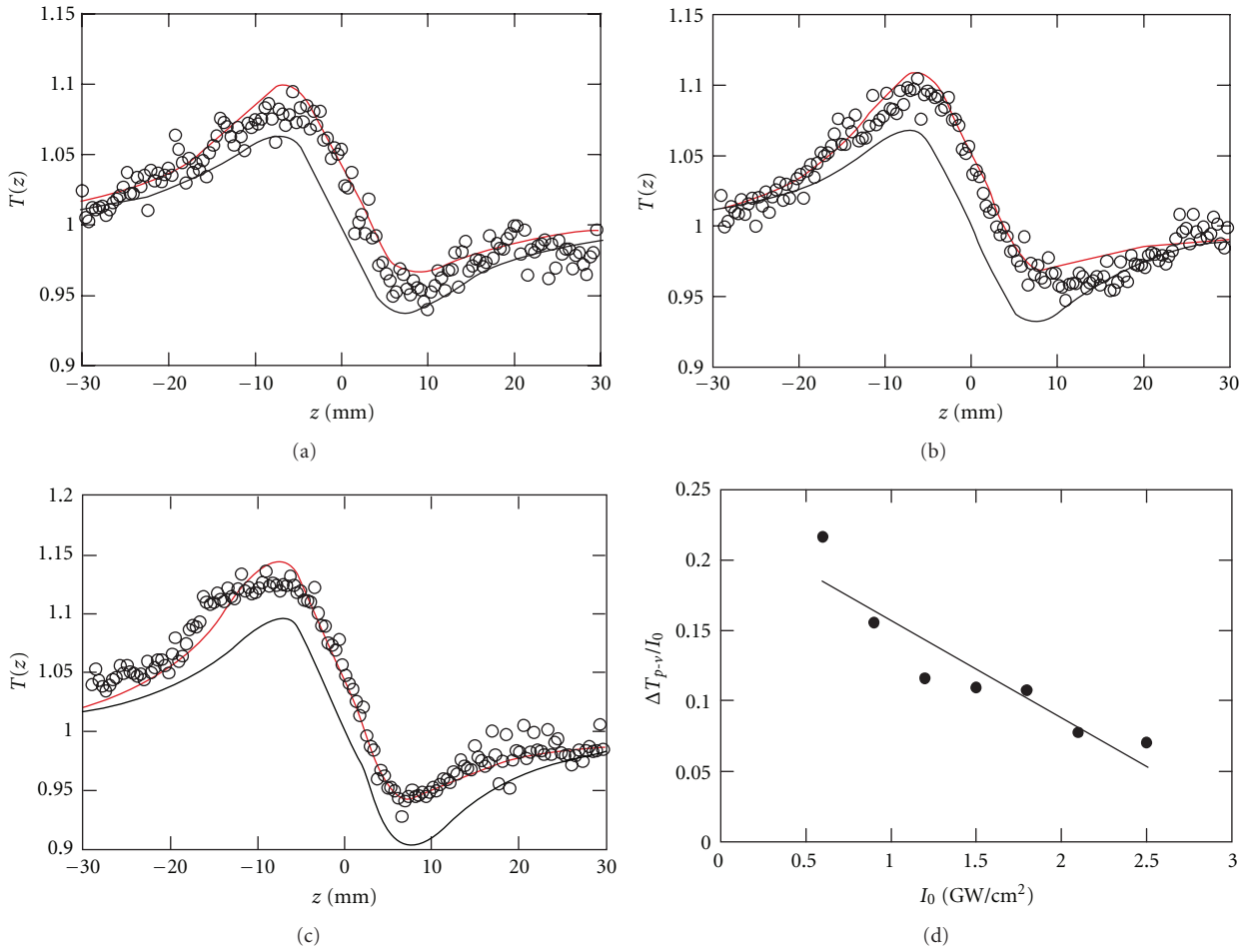

FIGURE 7: Closed-aperture Z-scan $T(z)$ at I_0 = (a) 0.6, (b) 1.2, and (c) 1.8 GW/cm^2 for the same film sample as that shown in Figure 5. Solid curves correspond to the least-squares fit of the theoretical formulae for the closed-aperture Z-scan with (red) and without (black) saturable absorption of a homogeneously broadened type. The best-fit values for n_2 and n_4 are $(-4.0 \pm 0.6) \times 10^{-3}$ cm^2/GW and $(1.5 \pm 0.4) \times 10^{-3}$ cm^4/GW^2, respectively. (d) $\Delta T_{p\text{-}v}/I_0$ as a function of input intensity I_0. The solid line is the least-squares linear fit to the data.

Acknowledgment

This work was supported by the Ministry of Education, Culture, Sports, Science, and Technology of Japan under Grant no. 20360030.

References

[1] M. Sheik-Bahae, A. A. Said, T. H. Wei, D. J. Hagan, and E. W. Van Stryland, "Sensitive measurement of optical nonlinearities using a single beam," *IEEE Journal of Quantum Electronics*, vol. 26, no. 4, pp. 760–769, 1990.

[2] R. L. Sutherland, *Handbook of Nonlinear Optics*, Marcel Dekker, New York, NY, USA, 2nd edition, 2003.

[3] B. Gu, J. Wang, J. Chen, Y. X. Fan, J. Ding, and H. T. Wang, "Z-scan theory for material with two- and three-photon absorption," *Optics Express*, vol. 13, no. 23, pp. 9230–9234, 2005.

[4] B. Gu, Y. X. Fan, J. Wang et al., "Characterization of saturable absorbers using an open-aperture Gaussian-beam Z scan," *Physical Review A*, vol. 73, no. 6, Article ID 065803, 2006.

[5] G. Tsigaridas, M. Fakis, I. Polyzos, M. Tsibouri, P. Persephonis, and V. Giannetas, "Z-scan analysis for near-Gaussian beams through Hermite-Gaussian decomposition," *Journal of the Optical Society of America B*, vol. 20, no. 4, pp. 670–676, 2003.

[6] G. Tsigaridas, M. Fakis, I. Polyzos, P. Persephonis, and V. Giannetas, "Z-scan analysis for high order nonlinearities through Gaussian decomposition," *Optics Communications*, vol. 225, no. 4–6, pp. 253–268, 2003.

[7] Z. Liu, W. Zang, J. Tian, W. Zhou, C. Zhang, and G. Zhang, "Analysis of Z-scan of thick media with high-order nonlinearity by variational approach," *Optics Communications*, vol. 219, no. 1–6, pp. 411–419, 2003.

[8] B. Gu, X. C. Peng, T. Jia, J. P. Ding, J. L. He, and H. T. Wang, "Determinations of third- and fifth-order nonlinearities by the use of the top-hat-beam Z scan: theory and experiment," *Journal of the Optical Society of America B*, vol. 22, no. 2, pp. 446–452, 2005.

[9] B. Gu, J. Chen, Y. X. Fan, J. Ding, and H. T. Wang, "Theory of Gaussian beam Z scan with simultaneous third- and fifth-order nonlinear refraction based on a Gaussian decomposition method," *Journal of the Optical Society of America B*, vol. 22, no. 12, pp. 2651–2659, 2005.

[10] X. Liu, Y. Tomita, J. Oshima et al., "Holographic assembly of semiconductor CdSe quantum dots in polymer for volume Bragg grating structures with diffraction efficiency near

100%," *Applied Physics Letters*, vol. 95, no. 26, Article ID 261109, 2009.

[11] X. Liu, Y. Tomita, J. Oshima, T. Nakashima, and T. Kawai, "High-order nonlinear optical response of a polymer nanocomposite film incorporating semiconducotor CdSe quantum dots," *Optics Express*, vol. 20, pp. 13457–13469, 2012.

[12] Y. Tomita, N. Suzuki, and K. Chikama, "Holographic manipulation of nanoparticle distribution morphology in nanoparticle-dispersed photopolymers," *Optics Letters*, vol. 30, no. 8, pp. 839–841, 2005.

[13] Y. Tomita, "Holographic manipulation of nanoparticle-distribution morphology in photopolymers and its applications to volume holographic recording and nonlinear photonic crystals," in *Proceedings of the OSA Trends in Optics and Photonics Series (TOPS '05)*, vol. 99, pp. 274–280, July 2005.

[14] R. E. Slusher and B. J. Eggleton, *Nonlinear Photonic Crystals*, Springer, Berlin, Germany, 2003.

[15] Y. Kayanuma, "Quantum-size effects of interacting electrons and holes in semiconductor microcrystals with spherical shape," *Physical Review B*, vol. 38, no. 14, pp. 9797–9805, 1988.

[16] S. Schmitt-Rink, D. A. B. Miller, and D. S. Chemla, "Theory of the linear and nonlinear optical properties of semiconductor microcrystallites," *Physical Review B*, vol. 35, no. 15, pp. 8113–8125, 1987.

[17] G. Banfi, V. Degiorgio, and D. Ricard, "Nonlinear optical properties of semiconductor nanocrystals," *Advances in Physics*, vol. 47, no. 3, pp. 447–510, 1998.

[18] L. H. Acioli, A. S. L. Gomes, and J. R. R. Leite, "Measurement of high-order optical nonlinear susceptibilities in semiconductor-doped glasses," *Applied Physics Letters*, vol. 53, no. 19, pp. 1788–1790, 1988.

[19] G. Banfi, V. Degiorgio, and H. M. Tan, "Optical nonlinearity of semiconductor-doped glasses at frequencies below the band gap: the role of free carriers," *Journal of the Optical Society of America B*, vol. 12, no. 4, pp. 621–628, 1995.

[20] K. S. Bindra and A. K. Kar, "Role of femtosecond pulses in distinguishing third- and fifth-order nonlinearity for semiconductor-doped glasses," *Applied Physics Letters*, vol. 79, no. 23, pp. 3761–3763, 2001.

[21] I. Dancus, V. I. Vlad, A. Petris, N. Gaponik, V. Lesnyak, and A. Eychmüller, "Saturated near-resonant refractive optical nonlinearity in CdTe quantum dots," *Optics Letters*, vol. 35, no. 7, pp. 1079–1081, 2010.

[22] Y. F. Chen, K. Beckwitt, F. W. Wise, B. G. Aitken, J. S. Sanghera, and I. D. Aggarwal, "Measurement of fifth- and seventh-order nonlinearities of glasses," *Journal of the Optical Society of America B*, vol. 23, no. 2, pp. 347–352, 2006.

[23] G. Adomian, "A review of the decomposition method in applied mathematics," *Journal of Mathematical Analysis and Applications*, vol. 135, no. 2, pp. 501–544, 1988.

[24] C. Burda, S. Link, T. C. Green, and M. A. El-Sayed, "New transient absorption observed in the spectrum of colloidal CdSe nanoparticles pumped with high-power femtosecond pulses," *Journal of Physical Chemistry B*, vol. 103, no. 49, pp. 10775–10780, 1999.

[25] M. Sheik-Bahae, D. C. Hutchings, D. J. Hagan, and E. W. Van Stryland, "Dispersion of bound electronic nonlinear refraction in solids," *IEEE Journal of Quantum Electronics*, vol. 27, no. 6, pp. 1296–1309, 1991.

[26] C. Gan, Y. Zhang, S. W. Liu, Y. Wang, and M. Xiao, "Linear and nonlinear optical refractions of CR39 composite with CdSe nanocrystals," *Optical Materials*, vol. 30, no. 9, pp. 1440–1445, 2008.

[27] K. Dolgaleva, H. Shin, and R. W. Boyd, "Observation of a microscopic cascaded contribution to the fifth-order nonlinear susceptibility," *Physical Review Letters*, vol. 103, no. 11, Article ID 113902, 2009.